Transitions between Rydberg states in two-color corotating circularly polarized laser pulses

Y. Gebre, J. Venzke, A. Jaron-Becker, and A. Becker
JILA and Department of Physics, University of Colorado, Boulder, Colorado 80309-0440, USA

(Received 24 July 2020; accepted 15 December 2020; published 5 January 2021)

We present a study of higher-order Raman (Λ, V, and S) transitions between Rydberg states involving the absorption and emission of at least three photons in the interaction of two-color corotating circularly polarized laser pulses with the hydrogen atom. Our analysis is based on results of numerical solutions of the corresponding time-dependent Schrödinger equation. The results for the interaction with (ω, 2ω) fields show that the simultaneous interaction with both fields results in an excited state distribution over a broad range of magnetic quantum numbers. Indications of the impact of the Λ, V, and S transitions are found via the analysis of final distributions resulting from the preparation of the atom in specific Rydberg states. Furthermore, we show that similar mechanisms for the redistribution of population between Rydberg states are present in two-color fields with larger differences in the central frequencies, i.e., (ω, 3ω) and (ω, 4ω) fields.

DOI: 10.1103/PhysRevA.103.013101

I. INTRODUCTION

The irradiation of atoms with two-color circularly polarized intense laser pulses has recently generated much interest in strong-field physics. The superposition of the two fields at different wavelengths with either co- or counterrotating polarization gives rise to optical wave forms much different from those of a single-color laser field. This results in new prospects and capabilities for fundamental strong-field processes, such as excitation, ionization, and high-order harmonic generation. For example, in high-order harmonic generation the application of a bicircular laser field has recently enabled the efficient phase-matched generation of circularly polarized harmonics at multiples of the driver wavelengths up to the extreme-ultraviolet and soft x-ray regimes [1–16], initially motivated by earlier work from about two decades ago [17,18]. In strong-field ionization by a bicircular laser pulse, the production of electron vortices [19,20] and spin-polarized electrons [21,22], the control of electron rescattering [23,24], the impact of excited states [25–27], the retrieval of target structure [28], the role of interferences [29,30], and the temporal resolution of the electron emission [31,32] have been analyzed.

The relative helicity of the two applied circularly polarized laser pulses has a significant effect on the manifold of accessible excited states during the interaction. Initially, it has been shown [25] that opposite photon polarization in counterrotating fields increases the probability for resonant-enhanced ionization as compared to the case of corotating fields. More recently, it has been studied [27] how the quantum selection rules for (multi-)photon absorption result in the selective population of excited states in atoms. Surprisingly, the results of the numerical simulations of the time-dependent Schrödinger equation in the case of corotating fields, however, also revealed population in states with orbital angular momentum and magnetic quantum numbers that are not accessible via sole absorption of photons from the two fields. It has been proposed that these states are populated via Raman-like transitions involving the absorption and emission of photons from both laser fields [27]. Let us assume without loss of generality that the two corotating fields have central frequencies ω and 2ω and are both left-handed circularly polarized, giving rise to selection rules of $\Delta m = -1$ for the absorption and $\Delta m = +1$ for the emission of a photon from either one of these fields. As shown in Fig. 1 (right column) the absorption of one photon at frequency 2ω (blue arrows) along with the emission of two photons at ω (red arrows) in a Λ, V, or S- results in a total change of magnetic quantum of $\Delta m = +1$. Analogously, photon emission at 2ω along with photon absorption at ω gives rise to $\Delta m = -1$ (Fig. 1, left column). Consequently, Λ, V, and S- can lead to a redistribution of population in Rydberg states, also beyond the manifold of states accessible by absorption only.

Changing and controlling the population in atomic energy levels via Λ and V transitions are well-known quantum mechanical processes which involve either one or two optical fields. Exemplary applications based on this phenomenon are coherent population trapping [33,34], inversion-free lasing [35], stimulated Raman adiabatic passage [36,37], electromagnetic-induced transparency [38,39], interference stabilization [40,41], and population trapping [42,43]. In all these applications the absorption and emission steps each involve one photon, i.e., in total a second-order process. In contrast the redistribution in the Rydberg states by corotating bicircular (ω, 2ω) laser fields relies on third-order processes requiring three photons, two at the longer wavelength and one at the shorter wavelength, leading to the transitions shown in Fig. 1.

The results of our previous study [27] indicated a redistribution during the population of Rydberg states by bicircular laser pulses, which can be controlled via the relative intensity of the two fields. In the present work we extend the analysis of the redistribution schemes. For our studies we make

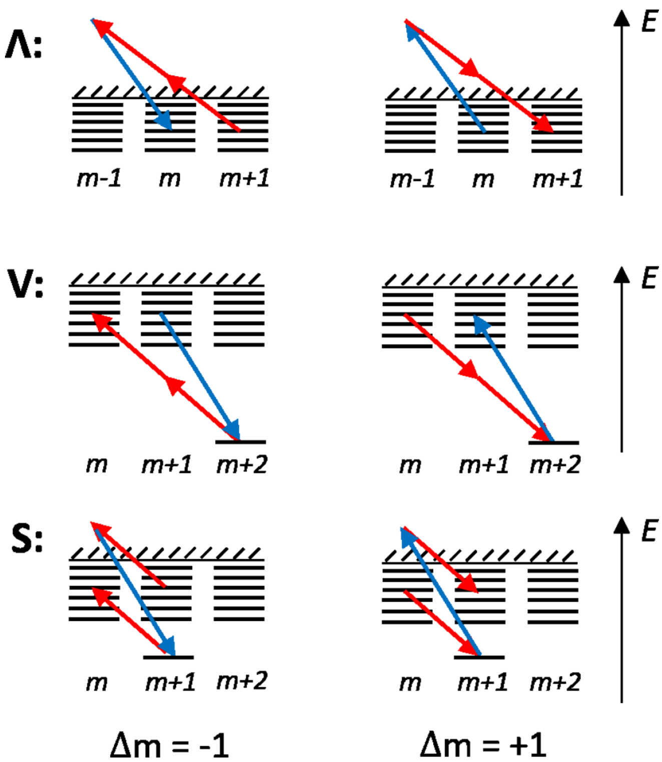

FIG. 1. Schemes for Λ (upper row), V (middle row), and S (lower row) transitions between Rydberg atomic states at central frequencies ω (red arrows) and 2ω (blue arrows) changing the magnetic quantum number by $\Delta m = -1$ (left panels) or $\Delta m = +1$ (right panels). The two applied corotating circularly polarized fields are assumed to be left-handed polarized.

use of results of numerical solutions of the time-dependent Schrödinger equation (TDSE) for the interaction of the hydrogen atom with intense bichromatic circularly polarized laser pulses. The paper is organized as follows: We first outline the methods used to solve the time-dependent Schrödinger equation and obtain the populations in the excited states in Sec. II. We then further establish the effects of the simultaneous presence of both fields on the excitation of atoms in corotating bicircular pulses at frequencies ω and 2ω in Sec. III A. By selecting the initial state of the atom in Sec. III B we analyze which kind of transitions are effective in the redistribution of population in the Rydberg states. In Sec. III C we provide indications that redistribution via even higher-order transitions occur in corotating circularly polarized fields with larger differences of the central frequencies. We end with a brief summary in Sec. IV.

II. NUMERICAL METHODS

We consider the interaction of the hydrogen atom with two circularly polarized intense laser pulses at different central frequencies ω_1 and ω_2. The corresponding TDSE in dipole approximation and velocity gauge is given by (we use Hartree atomic units $e = m_e = \hbar = 1$, if not stated otherwise) the following:

$$i\frac{\partial}{\partial t}\Psi(\mathbf{r},t) = \left[-\frac{\nabla^2}{2} - \frac{-i\mathbf{A}(t)\cdot\nabla}{c} - \frac{1}{r}\right]\Psi(\mathbf{r},t), \quad (1)$$

where $\mathbf{A}(t)$ is the total vector potential of the two laser pulses:

$$\mathbf{A}(t) = \mathbf{A}_{\omega_1}(t) + \mathbf{A}_{\omega_2}(t), \quad (2)$$

with

$$\mathbf{A}_\Omega(t) = A_{0,\Omega}\sin^2\left(\frac{\pi t}{\tau_\Omega}\right)[\sin(\Omega t)\hat{\mathbf{x}} + \epsilon_\Omega\cos(\Omega t)\hat{\mathbf{y}}] \quad (3)$$

for $\Omega = \omega_1$ and ω_2, respectively. $A_{0,\Omega} = \frac{c\sqrt{I_\Omega}}{\Omega}$, $\tau_\Omega = \frac{2\pi N_\Omega}{\Omega}$, and c is the speed of light, where I_Ω is the peak intensity and N_Ω denotes the number of cycles. Without loss of generalization, in our study we have chosen corotating left-handed circularly polarized pulses, i.e., $\epsilon_{\omega_1} = \epsilon_{\omega_2} = -1$.

To solve the TDSE numerically we expand the wave function Ψ in spherical harmonics up to $l_{\max} = 45$ and $m_{\max} = 45$. The radius is discretized using the fourth-order finite difference method with a grid spacing of 0.1 a.u. and a maximum radius of 750 a.u. with exterior complex scaling on the outer 38 a.u. of the grid. In time the wave function is propagated using the Crank-Nicolson method with a time step of 0.05 a.u. We have performed numerical calculations in which the central wavelength of one laser pulse is set at 267 nm, while the central wavelength of the second laser pulse is varied, namely, 534, 800, and 1068 nm. The number of cycles was chosen such that the pulse durations of the two pulses were the same. The initial state of the hydrogen atom was varied and the final state population was obtained by projecting the wave function at the end of the pulse onto the numerical bound ground and excited states on the grid.

III. RESULTS AND DISCUSSION

A. Population distribution in time-delayed bicircular corotating pulses

In the interaction with circularly polarized laser pulses the selection rules for the orbital angular momentum and magnetic quantum numbers limit the manifold of excited states accessible by absorption of photons [25,27]. In multiphoton absorption in each transition the magnetic quantum number is changed either by $\Delta m = +1$ (right-handed circular polarization) or $\Delta m = -1$ (left-handed circular polarization). In Fig. 2 we compare the distribution in the excited states of the hydrogen atom as a function of the magnetic quantum number (summed over n and ℓ with $n \geqslant 4$) by single circularly polarized pulses at 267 nm [panel (a)] and 534 nm [panel (b)] with that due to the interaction with the superposition of the two pulses [panel (c)]. The pulse durations of the two pulses were chosen to be the same and in the superposition the maxima of the field were chosen to coincide.

The distributions induced by the individual pulses are limited to narrow ranges in m, in agreement with the excitation via absorption of three photons at 267 nm and six or seven photons at 534 nm. The total photon energies at the central frequency are 13.92 eV (three photons at 267 nm and six photons at 534 nm) and 16.24 eV (seven photons at 534 nm). Assuming that the Rydberg states approximatively shift with the ponderomotive energy, which is 0.333 eV (267 nm, 5×10^{13} W/cm^2) and 2.663 eV (534 nm, 1×10^{14} W/cm^2) at peak intensity, respectively, the maxima of the population distributions are in agreement with an excitation near the center of the pulse.

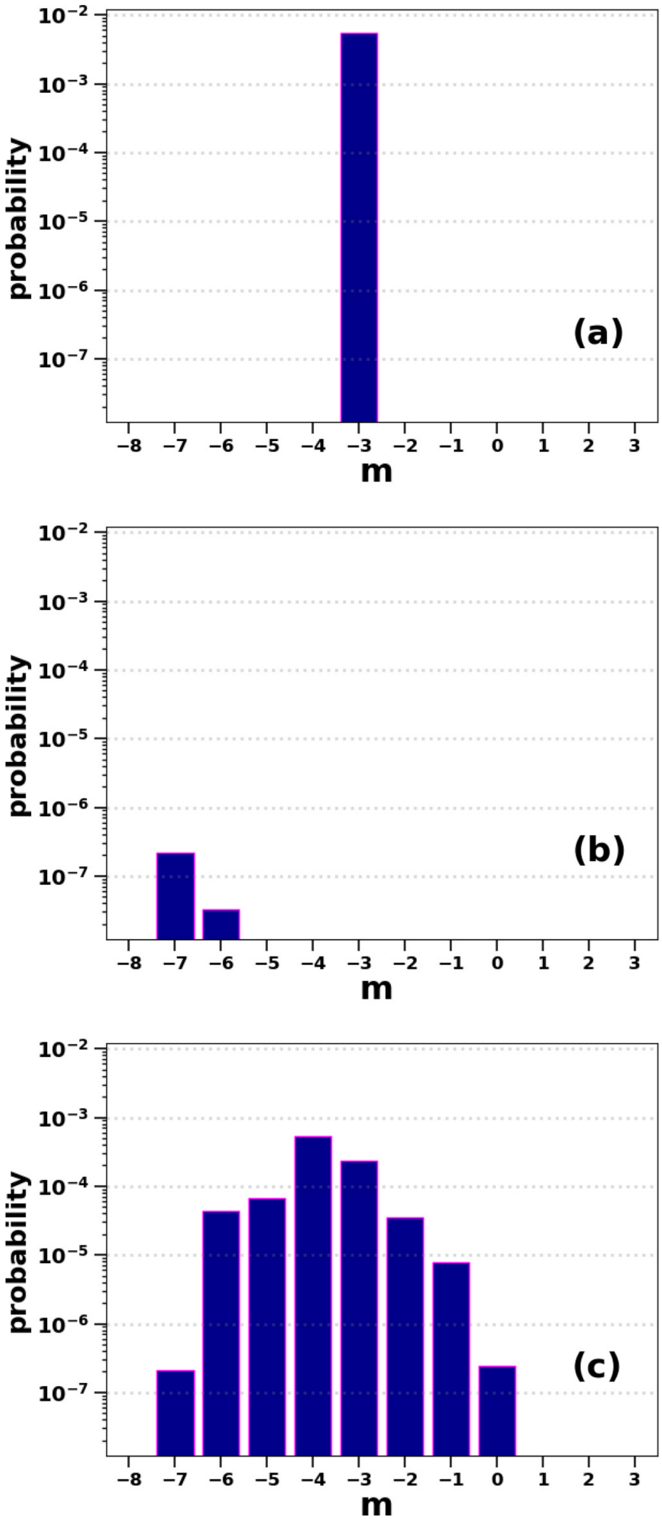

FIG. 2. Comparison of excited state distributions as a function of the magnetic quantum number m (summed over n and ℓ with $n \geqslant 4$) for excitation with (a) a circularly polarized laser pulse at 267 nm (20 cycles, 5×10^{13} W/cm^2), (b) a circularly polarized laser pulse at 534 nm (10 cycles, 1×10^{14} W/cm^2), and (c) a corotating bicircular laser pulse.

In contrast, the distribution is much broader for the interaction with the bicircular laser pulse. The states with magnetic quantum numbers between $m = -3$ and $m = -7$ are accessible via the combined absorption of photons from both fields. However, the results also reveal population in states with $m > -3$, which cannot be populated just via photon absorption alone. We have previously proposed [27] that a redistribution of population between Rydberg states with different magnetic quantum numbers via Raman-type transitions involving three photons (cf., Fig. 1) is effective when both pulses are present.

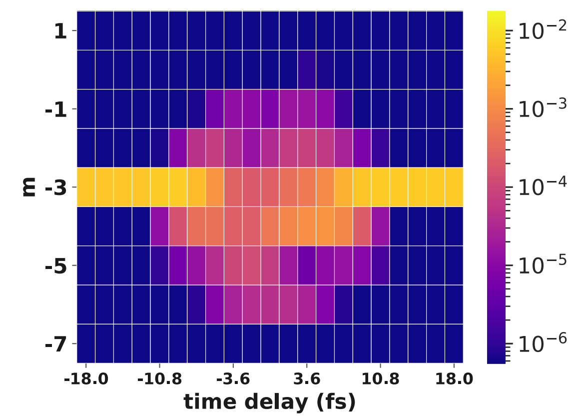

FIG. 3. Excitation probability in states with the magnetic quantum number m (summed over n and ℓ with $n \geqslant 4$) for two corotating circularly polarized pulses at 267 nm (20 cycles, 5×10^{13} W/cm^2) and 534 nm (10 cycles, 1×10^{14} W/cm^2) as a function of time delay between the pulses. At negative (positive) time delays the 267-nm (534-nm) pulse precedes.

The interpretation that the populations in the states outside of $m = -3$ are only populated when both pulses overlap in time is confirmed by the results in Fig. 3, which show the population distributions as a function of the magnetic quantum number and the time delay between the two pulses. The pulse parameters were kept the same as for the simulations in Fig. 2(c). When the pulses do not overlap, i.e., for delays $|\Delta t| > 11$ fs, the population is concentrated in $m = -3$ in agreement with an excitation by the 267-nm laser pulse without impact of the preceding (positive time delays) or subsequent (negative time delays) 534-nm laser pulse. In contrast, once the pulses overlap in time there appears population in states with m values larger and smaller than -3. Furthermore, the range in m over which the population extends, as well as the magnitude of population outside of $m = -3$ itself, gets larger the more the pulses overlap.

B. Transitions between Rydberg states

The results so far indicate that the simultaneous presence of both pulses is required for the population of excited states with magnetic quantum numbers other than $m = -3$ (and $m = -6$ and -7). Next, we analyze if any of the transitions for the redistribution between Rydberg states, shown in Fig. 1, are effective mechanisms in the bicircular pulse. To this end, we consider that the hydrogen atom is initially prepared in a specific Rydberg state. While the processes can proceed via virtual states, the transition probabilities are larger when intermediate real states are involved. For two of the transitions (V and S) there is first an emission of one or two photons at the smaller photon energy and, hence, intermediate bound states

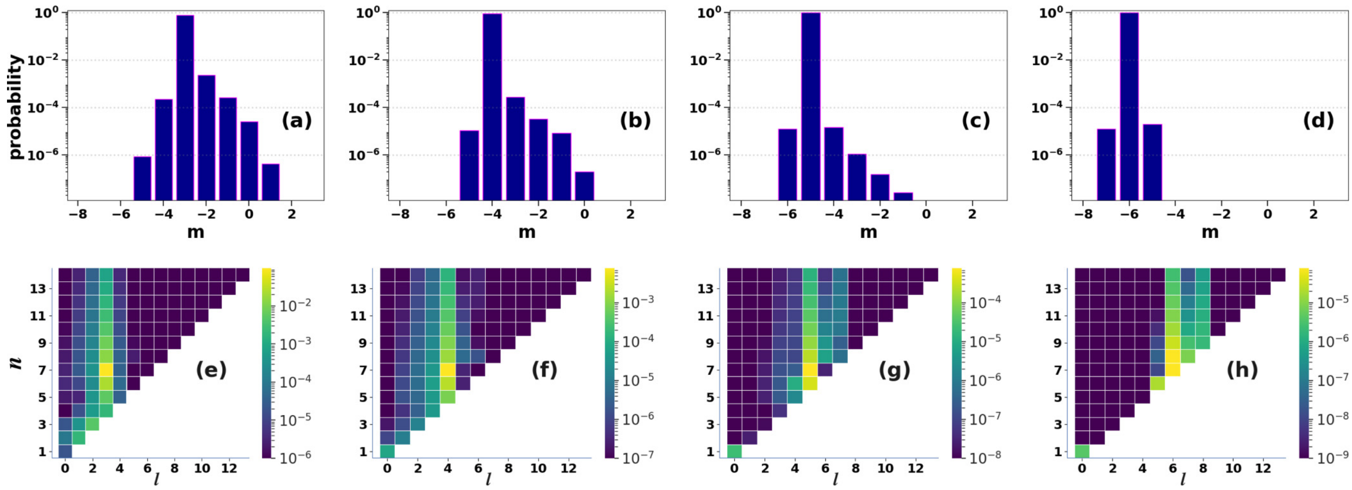

FIG. 4. Excitation probability as a function of the magnetic quantum number (summed over n and ℓ with $n \geqslant 4$, upper row) and as function of principal and orbital angular momentum quantum numbers (summed over m, lower row) for two corotating circularly polarized pulses at 267 nm (20 cycles, 5×10^{13} W/cm^2) and 534 nm (10 cycles, 1×10^{14} W/cm^2). Results are obtained for initial states prepared in $n_0 = 7$ and $\ell_0 = 3$, $m_0 = -3$ (a), (e); $\ell_0 = 4$, $m_0 = -4$ (b), (f); $\ell_0 = 5$, $m_0 = -5$ (c), (g); and $\ell_0 = 6$, $m_0 = -6$ (d), (h).

at lower energies must be accessible to make the transition effective. Furthermore, we expect that there remains some population in these lower-lying states at the end of the pulse.

For the V mechanism [Fig. 1(b)] the transition to the lowest intermediate state is associated with an energy exchange of $\Delta E = -2\omega \approx -4.64$ eV (for the bicircular pulse used in the present analysis), and $\Delta m = +1$ (for a total change of $\Delta m = -1$) or $\Delta m = +2$ (for a total change of $\Delta m = +1$). Assuming that the initial Rydberg state shifts with the ponderomotive energy during the pulse while the lowest-lying intermediate states may shift less in energy, the states at the $n = 2$ level in the hydrogen atom must be accessible for the V transition to be effective. Similarly, the S transition to the lower intermediate state is associated with $\Delta E = -\omega \approx -2.32$ eV and $\Delta\ell = \Delta m = +1$ (for a total change in m of $+1$ or -1). Therefore, it is most likely that the transition occurs via states at the $n = 3$ level. Due to the restriction in orbital angular momentum ($\ell < n$) and magnetic quantum numbers ($|m| < n$) the accessibility of the intermediate lower-lying states depends on the quantum numbers of the initially prepared Rydberg state, which allows us to test the presence of the redistribution mechanisms proposed in Fig. 1.

To this end we have performed a series of calculations in which initially the hydrogen atom is prepared in specific Rydberg states, namely ($n_0 = 7$, $\ell_0 = 3$, $m_0 = -3$) to ($n_0 = 7$, $\ell_0 = 6$, $m_0 = -6$), changing ℓ_0 by 1 and m_0 by -1. The distributions as functions of magnetic quantum numbers and as functions of principal and orbital angular momentum quantum numbers at the end of the interaction with the same bicircular pulse as in Fig. 2(c) are presented in Fig. 4. The population in states with magnetic quantum numbers larger than that of the initial state clearly depends on the choice of the initial state. While for $\ell_0 = 3$ and $m_0 = -3$ there is a redistribution over a range of states up to $m = 1$, the range gets smaller as ℓ_0 (smaller m_0) of the initial state increases. The ranges of the distributions indicate that for most of the cases there is a sequence of transitions occurring. In general, the type of transition (Λ, V, S) may change from step to step in the sequence.

For the initial state $\ell_0 = 3$ and $m_0 = -3$ [Figs. 4(a) and 4(e)], the total change in m is 4, indicating a sequence of up to four transitions. Any of the final states, except those with $m = 1$, can be accessed by any one of the three transitions shown in Fig. 1. For the V transition the process likely proceeds via $n = 2$ states with $\ell = -1$, 0, and 1, and this transition is therefore not resonant for the final step into the $m = 1$ states, since the required intermediate state with $m = 2$ does not exist in the $n = 2$ manifold of states. The other two pathways (Λ and S) are both allowed for each transition in the sequence. Another indication that the V and S pathways are effective in the redistribution is the remaining populations in the intermediate ($n = 2$, $\ell = 1$) and ($n = 3$, $\ell = 2$) states of these pathways at the end of the pulse.

For the next initial state [$\ell_0 = 4$, $m_0 = -4$; Figs. 4(b) and 4(f)], the range of populated m states indicates again a sequence of up to four transitions. In this case it is, however, unlikely that the first transition in the sequence to $m = -3$ occurs via the V or S pathway since the required intermediate states with $m = -3$ (in the $n = 3$ manifold) and $m = -2$ states (in the $n = 2$ manifold) do not exist. This agrees with the reduced overall probability of redistribution over the Rydberg states with magnetic quantum numbers larger than that of the initial state as well as with the lower population in the intermediate states ($n = 2$ and 3) required for the V and S transitions in the sequence beyond the first step.

The trend of reduced probability in the redistribution to states with larger magnetic quantum numbers continues as the quantum numbers of the initial state are changed to larger absolute values in ℓ_0 and m_0. In the final example considered ($\ell_0 = 6$, $m_0 = -6$; Figs. 4(d) and 4(h)], the transfer of population to the $m = -5$ state can occur via the Λ pathway only. This pathway, however, appears to be effective for just one step in the change of the magnetic quantum number with rather low probability only. This may indicate that the V and S transitions via bound states with lower energy are overall more probable than the Λ transition via the continuum states in the redistribution of population between Rydberg states.

The last part of our interpretation about the relative efficiency of the different types of transitions agrees with the observations for the redistribution into states with magnetic quantum numbers smaller than that of the initial state. Except for the ($\ell_0 = 3$, $m_0 = -3$) initial state, the V and S transitions are not open for a change of $\Delta m = -1$ since the required intermediate states in the $n = 2$ and $n = 3$ manifolds do not exist. Due to the restriction in pathways we observe population in just one (or two) states with smaller magnetic quantum numbers. Since the Λ transition is the only $\Delta m = -1$ pathway for all initial states with $\ell_0 \geqslant 4$, the results confirm that the probability for this transition is small and independent of the values of the orbital angular momentum and magnetic quantum numbers.

There are a few more interesting features in the (n, ℓ) distributions in Fig. 4 (lower row), which we will discuss now. These features are not closely related to the main focus of the article, namely, the three-photon Λ, V, and S transitions involving both fields. First, we note that the final distributions in the ℓ_0 channel are spread over all available principal quantum numbers n. We interpret this result primarily as an indication of the presence of one-pulse Λ transitions through the continuum, consisting of the absorption of a photon followed by the emission of one photon from one of the two fields. In these transitions the changes in orbital angular momentum and magnetic quantum number are given by $\Delta\ell = 0$ and ± 2 and $\Delta m = 0$. Therefore, the population in the $\ell_0 + 2$ channels in some of the final distributions is another indicator for the presence of these kinds of transitions. This process was previously analyzed in the context of interference stabilization [40,41] and population trapping [42,43] in strong fields. In the final distributions we further note the population in the ground state. Each of the initial Rydberg states considered in this set of calculations is within the manifold of states that can be reached from the ground state via sole absorption of photons from the two fields. Therefore, it is likely that the ground-state population is due to the inverse process, namely, the deexcitation from the initial Rydberg state via the stimulated emission of photons.

C. Higher-order transitions in (ω, $p\omega$) corotating circularly polarized pulses

The population of Rydberg states with magnetic quantum numbers in corotating bicircular $(\omega, 2\omega)$ fields that are not accessible via absorption of photons from the initial states raises the question if similar distributions occur in corotating circularly polarized $(\omega, p\omega)$ fields with $p > 2$ as well. To answer this question we have performed additional calculations for the superposition of one pulse at 267 nm and a second pulse at 800 and 1068 nm, respectively. In each case the pulse durations of the two pulses were chosen to be same and the centers of the pulses were chosen to coincide. The pulses at the longer wavelength had a peak intensity of 1×10^{14} W/cm^2, while the peak intensity of the 267-nm pulse was 5×10^{13} W/cm^2, as in the $(\omega, 2\omega)$ studies above. In test calculations we have found that sole application of each of the pulses at the long wavelengths does not produce any significant population in the excited states.

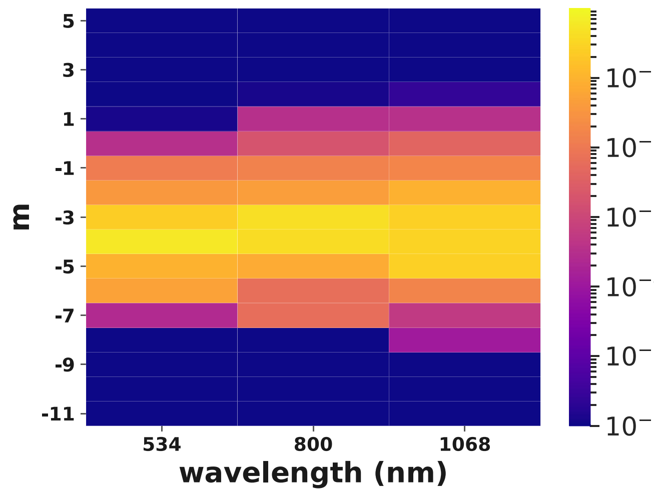

FIG. 5. Comparison of normalized excitation probabilities in states with the magnetic quantum number m (summed over n and ℓ with $n \geqslant 4$) for two corotating circularly polarized pulses at 267 nm (30 cycles, 5×10^{13} W/cm^2), 534 nm (15 cycles, 1×10^{14} W/cm^2), 800 nm (10 cycles, 1×10^{14} W/cm^2), and 1068 nm (7.5 cycles, 1×10^{14} W/cm^2).

From the comparison of the results for the normalized excitation probabilities as a function of the magnetic quantum number at the end of the pulse with that of the $(\omega, 2\omega)$ case in Fig. 5, it is seen that the range of states as a function of the magnetic quantum number and the relative redistribution probability increase with changes from $p = 2$ to $p = 4$. Thus, higher-order transitions involving the emission and absorption of more than three photons are likely effective in the excitation of hydrogen atoms with $(\omega, p\omega)$ fields. The number of possible pathways increases with increases of p, and changes in the magnetic quantum number up to $\Delta m = \pm(p - 1)$ are possible in the individual transitions.

As in the case of the $(\omega, 2\omega)$ field, we have performed additional series of calculations by preparing the hydrogen atom in specific Rydberg states. The final distributions over the magnetic quantum numbers for the interaction with the superposition of corotating left-handed circularly polarized fields at 267 and 800 nm are shown in Fig. 6. The distributions are obtained for initial states ranging from ($n_0 = 10$, $\ell_0 = 3$, $m_0 = -3$) to ($n_0 = 10$, $\ell_0 = 9$, $m_0 = -9$), changing ℓ_0 by 2 and m_0 by -2. The distributions show the same trends as those in Fig. 4. The range of populated magnetic quantum states decreases and the overall redistribution probability over the Rydberg states decreases as ℓ_0 increases (smaller m_0). These features indicate that an interpretation similar to that for the $(\omega, 2\omega)$ field holds. As ℓ_0 increases, transitions that involve photons from both fields and that proceed via lower-lying states are stepwise excluded, which provides an explanation for the observed features.

IV. SUMMARY

We have studied the distribution of population in Rydberg states induced by the superposition of two-color corotating circularly polarized laser fields. Using the solutions of the time-dependent Schrödinger equation it is shown that the

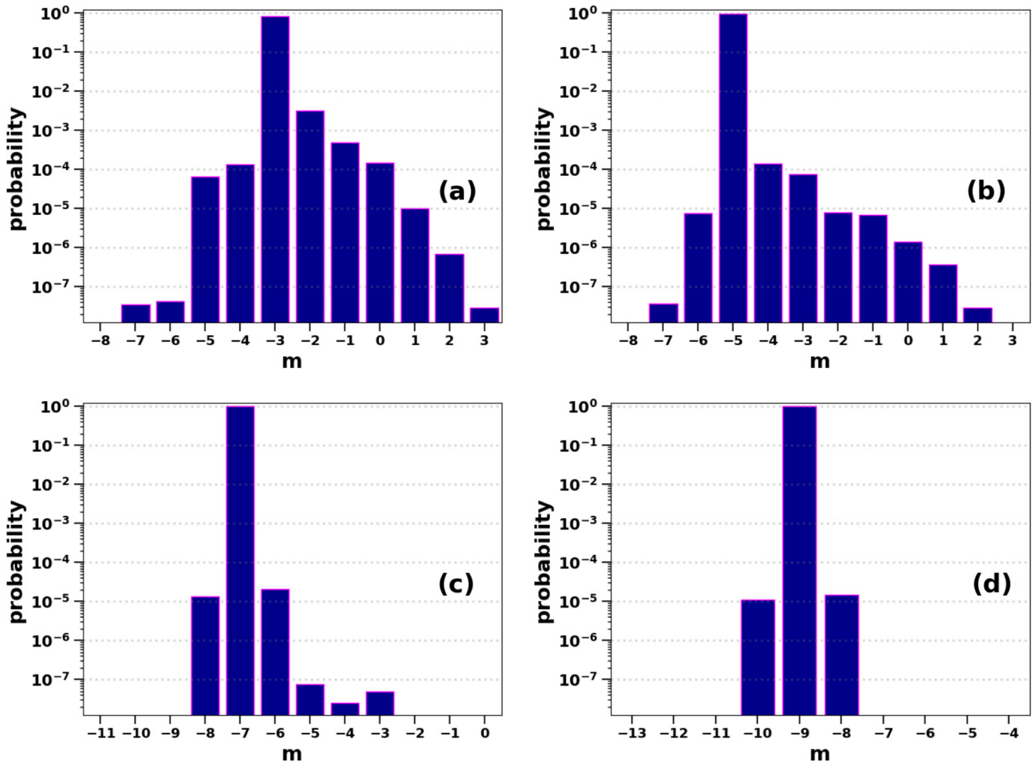

FIG. 6. Excitation probability as a function of magnetic quantum number (summed over n and ℓ with $n \geqslant 4$) and as a function of principal and orbital angular momentum quantum numbers (summed over m, lower row) for two corotating circularly polarized pulses at 267 nm (30 cycles, 5×10^{13} W/cm^2) and 800 nm (10 cycles, 1×10^{14} W/cm^2). Results are obtained for initial states prepared in $n_0 = 10$ and $\ell_0 = 3$, $m_0 = -3$ (a); $\ell_0 = 5$, $m_0 = -5$ (b); $\ell_0 = 7$, $m_0 = -7$ (c); and $\ell_0 = 9$, $m_0 = -9$ (d).

simultaneous interaction with both fields leads to a distribution in states over a broad range of magnetic quantum numbers, in contrast to narrow distributions if only one of the two fields is present. Since the range extends beyond that accessible via absorption of photons from the two fields, we have proposed that higher-order Raman (Λ, V, S) transitions, involving absorption and emission of at least three photons from the two fields, are effective mechanisms in the redistribution of population between Rydberg states.

By selecting specific Rydberg states in the numerical calculations it has been found that the distributions over the orbital angular momentum and magnetic quantum numbers depend on the initial state. The changes in the distributions have been interpreted as indications of the presence of the higher-order Raman transitions. Specifically, the elimination of the V and S pathways via lower-lying states leads to a significant decrease in the overall redistribution probability and the range of populated ℓ and m states in the final distribution.

While the presence of the proposed transitions is supported by the present results, we note that the overall excitation and redistribution probabilities are rather low. This is related to the fact that the competing process of ionization, i.e., transitions to the continuum, has a much higher probability. Indeed, in all calculations presented in this work the ionization probability is typically by a couple of orders of magnitude larger than the total redistributed excitation probability. It is likely that the ratio between excitation and ionization can be controlled to some degree via the various laser parameters, such as the intensity ratio (as shown in Ref. [27]), the relative wavelengths, the relative carrier-to-envelope phase, and the pulse durations of the two fields as well as the time delay in between them. This is, however, beyond the scope of the present work, in which we have provided an analysis of the basic mechanisms behind the redistribution. Although the efficiency of the control may be limited in view of the number of competing pathways (ionization, direct excitation, and Λ, V, and S transitions), we note that the impact of the carrier-to-envelope phase on bound-bound transitions [44,45] and coherent control protocols to prepare specific Rydberg states [46,47] have been studied recently. To this end, it can be useful to further analyze qualitatively and quantitatively each of the transitions separately using other theoretical approaches, e.g., via lowest-order perturbation theory.

Finally, we have shown that redistribution mechanisms are also present in $(\omega, 3\omega)$ and $(\omega, 4\omega)$ fields. The range of populated m states increases as the difference in the central frequencies of the two fields gets larger. This is in agreement with the increase in the change of magnetic quantum numbers in higher-order Raman transitions in $(\omega, p\omega)$ fields with $p > 2$. Results of calculations starting from specific initial Rydberg states support the conclusions drawn for the $(\omega, 2\omega)$ case.

ACKNOWLEDGMENTS

This work was primarily supported (Y.G., J.V., A.B.) by a grant from the U.S. Department of Energy, Division of

Chemical Sciences, Atomic, Molecular and Optical Sciences Program (Grant No. DE-SC0001771). A.J.-B. acknowledges support by a grant from the U.S. National Science Foundation (Grant No. PHY-1734006).

[1] A. Fleischer, O. Kfir, T. Diskin, P. Sidorenko, and O. Cohen, Nat. Photonics **8**, 543 (2014).
[2] O. Kfir, P. Grychtol, E. Turgut, R. Knut, D. Zusin, D. Popmintchev, T. Popmintchev, H. Nembach, J. M. Shaw, A. Fleischer *et al.*, Nat. Photonics **9**, 99 (2015).
[3] T. Fan, P. Grychtol, R. Knut, C. Hernández-García, D. D. Hickstein, D. Zusin, C. Gentry, F. J. Dollar, C. A. Mancuso, C. W. Hogle *et al.*, Proc. Natl. Acad. Sci. USA **112**, 14206 (2015).
[4] D. D. Hickstein, F. J. Dollar, P. Grychtol, J. L. Ellis, R. Knut, C. Hernández-García, D. Zusin, C. Gentry, J. M. Shaw, T. Fan *et al.*, Nat. Photonics **9**, 743 (2015).
[5] L. Medišauskas, J. Wragg, H. van der Hart, and M. Y. Ivanov, Phys. Rev. Lett. **115**, 153001 (2015).
[6] D. B. Milošević, Opt. Lett. **40**, 2381 (2015).
[7] C. Chen, Z. Tao, C. Hernández-García, P. Matyba, A. Carr, R. Knut, O. Kfir, D. Zusin, C. Gentry, P. Grychtol *et al.*, Sci. Adv. **2**, e1501333 (2016).
[8] D. Baykusheva, M. S. Ahsan, N. Lin, and H. J. Wörner, Phys. Rev. Lett. **116**, 123001 (2016).
[9] C. Hernández-García, C. G. Durfee, D. D. Hickstein, T. Popmintchev, A. Meier, M. M. Murnane, H. C. Kapteyn, I. J. Sola, A. Jaron-Becker, and A. Becker, Phys. Rev. A **93**, 043855 (2016).
[10] D. M. Reich and L. B. Madsen, Phys. Rev. Lett. **117**, 133902 (2016).
[11] K. M. Dorney, J. L. Ellis, C. Hernández-García, D. D. Hickstein, C. A. Mancuso, N. Brooks, T. Fan, G. Fan, D. Zusin, C. Gentry, P. Grychtol, H. C. Kapteyn, and M. M. Murnane, Phys. Rev. Lett. **119**, 063201 (2017).
[12] N. Zhavoronkov and M. Ivanov, Opt. Lett. **42**, 4720 (2017).
[13] D. Baykusheva, S. Brennecke, M. Lein, and H. J. Wörner, Phys. Rev. Lett. **119**, 203201 (2017).
[14] G. Lerner, T. Diskin, O. Neufeld, O. Kfir, and O. Cohen, Opt. Lett. **42**, 1349 (2017).
[15] L. Barreau, K. Veyrinas, V. Gruson, S. J. Weber, T. Auguste, J.-F. Hergott, F. Lepetit, B. Carré, J.-C. Houver, D. Dowek *et al.*, Nat. Commun. **9**, 4727 (2018).
[16] P.-C. Huang, C. Hernández-García, J.-T. Huang, P.-Y. Huang, C.-H. Lu, L. Rego, D. D. Hickstein, J. L. Ellis, A. Jaron-Becker, A. Becker *et al.*, Nat. Photonics **12**, 349 (2018).
[17] H. Eichmann, A. Egbert, S. Nolte, C. Momma, B. Wellegehausen, W. Becker, S. Long, and J. K. McIver, Phys. Rev. A **51**, R3414(R) (1995).
[18] S. Long, W. Becker, and J. K. McIver, Phys. Rev. A **52**, 2262 (1995).
[19] J. M. Ngoko Djiokap, S. X. Hu, L. B. Madsen, N. L. Manakov, A. V. Meremianin, and A. F. Starace, Phys. Rev. Lett. **115**, 113004 (2015).
[20] D. Pengel, S. Kerbstadt, D. Johannmeyer, L. Englert, T. Bayer, and M. Wollenhaupt, Phys. Rev. Lett. **118**, 053003 (2017).
[21] D. B. Milošević, Phys. Rev. A **93**, 051402(R) (2016).
[22] M.-M. Liu, Y. Shao, M. Han, P. Ge, Y. Deng, C. Wu, Q. Gong, and Y. Liu, Phys. Rev. Lett. **120**, 043201 (2018).
[23] C. A. Mancuso, D. D. Hickstein, K. M. Dorney, J. L. Ellis, E. Hasović, R. Knut, P. Grychtol, C. Gentry, M. Gopalakrishnan, D. Zusin, F. J. Dollar, X. M. Tong, D. B. Milosevic, W. Becker, H. C. Kapteyn, and M. M. Murnane, Phys. Rev. A **93**, 053406 (2016).
[24] K. Lin, X. Jia, Z. Yu, F. He, J. Ma, H. Li, X. Gong, Q. Song, Q. Ji, W. Zhang *et al.*, Phys. Rev. Lett. **119**, 203202 (2017).
[25] C. A. Mancuso, K. M. Dorney, D. D. Hickstein, J. L. Chaloupka, X.-M. Tong, J. L. Ellis, H. C. Kapteyn, and M. M. Murnane, Phys. Rev. A **96**, 023402 (2017).
[26] P. Stammer, S. Patchkovskii, and F. Morales, Phys. Rev. A **101**, 033405 (2020).
[27] J. Venzke, Y. Gebre, A. Becker, and A. Jaron-Becker, Phys. Rev. A **101**, 053425 (2020).
[28] V.-H. Hoang, V.-H. Le, C. D. Lin, and A.-T. Le, Phys. Rev. A **95**, 031402(R) (2017).
[29] S. Eckart, M. Kunitski, I. Ivanov, M. Richter, K. Fehre, A. Hartung, J. Rist, K. Henrichs, D. Trabert, N. Schlott, L. P. H. Schmidt, T. Jahnke, M. S. Schoffler, A. Kheifets, and R. Dorner, Phys. Rev. A **97**, 041402(R) (2018).
[30] M. Han, P. Ge, Y. Shao, Q. Gong, and Y. Liu, Phys. Rev. Lett. **120**, 073202 (2018).
[31] N. Eicke and M. Lein, Phys. Rev. A **99**, 031402 (2019).
[32] P. Ge, M. Han, Y. Deng, Q. Gong, and Y. Liu, Phys. Rev. Lett. **122**, 013201 (2019).
[33] E. Arimondo and G. Orriols, Lett. Nuovo Cimento (1971–1985) **17**, 333 (1976).
[34] H. R. Gray, R. M. Whitley, and C. R. Stroud, Opt. Lett. **3**, 218 (1978).
[35] A. Imamoğlu and S. E. Harris, Opt. Lett. **14**, 1344 (1989).
[36] U. Gaubatz, P. Rudecki, S. Schiemann, and K. Bergmann, J. Chem. Phys. **92**, 5363 (1990).
[37] P. Marte, P. Zoller, and J. L. Hall, Phys. Rev. A **44**, R4118(R) (1991).
[38] K.-J. Boller, A. Imamoğlu, and S. E. Harris, Phys. Rev. Lett. **66**, 2593 (1991).
[39] J. E. Field, K. H. Hahn, and S. E. Harris, Phys. Rev. Lett. **67**, 3062 (1991).
[40] M. V. Fedorov and A. M. Movsesian, J. Phys. B: At., Mol. Opt. Phys. **21**, L155 (1988).
[41] M. V. Fedorov, M.-M. Tehranchi, and S. M. Fedorov, J. Phys. B: At., Mol. Opt. Phys. **29**, 2907 (1996).
[42] A. Talebpour, C.-Y. Chien, and S. L. Chin, J. Phys. B: At., Mol. Opt. Phys. **29**, 5725 (1996).
[43] A. Talebpour, Y. Liang, and S. L. Chin, J. Phys. B: At., Mol. Opt. Phys. **29**, 3435 (1996).
[44] D. Peng, B. Wu, P. Fu, B. Wang, J. Gong, and Z.-C. Yan, Phys. Rev. A **82**, 053407 (2010).
[45] Z. Zhai, D. Peng, X. Zhao, F. Guo, Y. Yang, P. Fu, J. Chen, Z.-C. Yan, and B. Wang, Phys. Rev. A **86**, 043432 (2012).
[46] S. Patsch, D. M. Reich, J.-M. Raimond, M. Brune, S. Gleyzes, and C. P. Koch, Phys. Rev. A **97**, 053418 (2018).
[47] J. Solanpää and E. Räsänen, Phys. Rev. A **98**, 053422 (2018).